Supporting Information: Bandgap Tunability in Partially Amorphous Silicon Nanoparticles Using Single-Dot Correlative Microscopy

Chia-Ching Huang,[†] Yingying Tang,[†] Marco van der Laan,[†] Jorik van de Groep,[†] A. Femius Koenderink,[†,‡] and Kateřina Dohnalová[*,†]

[†]*Institute of Physics, University of Amsterdam, Science Park 904, 1098 XH Amsterdam, the Netherlands*

[‡]*Center for Nanophotonics, AMOLF, Science Park 104, 1098 XG Amsterdam, the Netherlands*

E-mail: k.newell@uva.nl

Setup methodology of correlative optical microscopy with AFM

The major challenge of the correlative AFM and PL microscopy is the nanometer precision alignment of the optical microscopy system with the coupled AFM system, to allow measurement of one and the same single Si-NP in both systems simultaneously. For this, we use purely optical correlation, where we align the coordinates of both microscopes in several steps. First, alignment of the tip is done using a 20× objective lens. The area scanned by the tip can be at this stage roughly aligned with the field-of-view (FOV) of the optical imaging system by allowing the tip to move along the scanning area's boundary, where the movement of the tip is visible on the CCD detector. Independent tip and sample scanning modes allow us to move the tip independently with respect to the imaging objective lens. To calibrate the orientation, positioning, and size of the scanned FOV areas in both systems, we measure first a reference cross with 10-μm features (Ted Pella, Inc.). The major challenge arises due to the manual placement of the AFM tip, which is not reproducible with high precision. Also, switching from the 20× objective lens, used for the rough tip alignment, to the 100× objective lens, used for the spectroscopy, introduces an uncertainty between coarse and fine alignment of about ¡ 3 μm due to a shift in the focal plane and poor visibility of the large AFM cantilever in the smaller FOV. However, since the operation range of the TAO stage is 100×100 μm^2, we can re-align the position of the 80×80 μm^2 optical FOV comfortably. Thus we adjust for the ¡ 3-μm error. An alternative solutions could be pre-patterning of the substrate, however, such procedure would be expensive and would only introduce laser scattering and possibly mechanical damage to the originally smooth substrate, which could result in undesired emission background.

Additional spectroscopy data

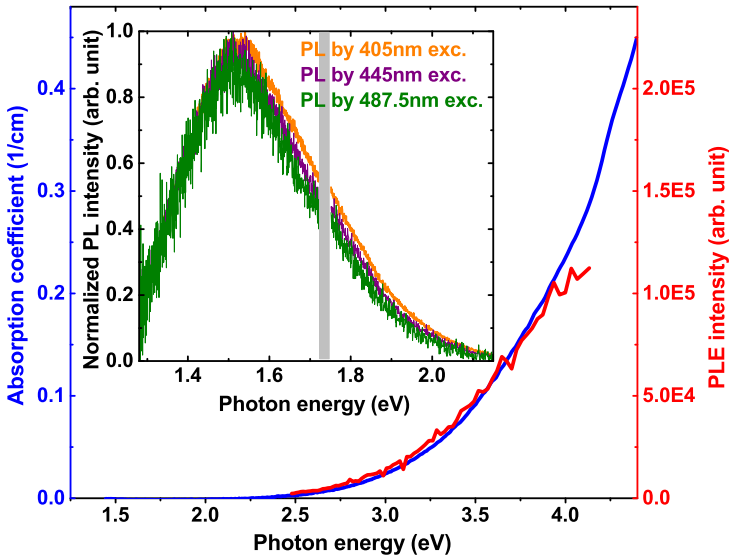

Figure S1: Extinction (blue line) and PLE (red line) spectrum of the Si-NPs dispersed in toluene. PLE is measured for PL peak at 813 nm (1.53 eV). Inset: PL spectra of Si-NPs ensemble excited by a Xe lamp at 405 (3.06 eV, orange line), 445 (2.79 eV, purple line) and 487.5 nm (2.54 eV, green line) in the PLE setup. PL spectra peak at 809 (1.53 eV), 813 (1.53 eV) and 816 nm (1.52 eV), respectively. The gray region shows the discontinuity caused by switching between two different gratings in the detection spectrometer.

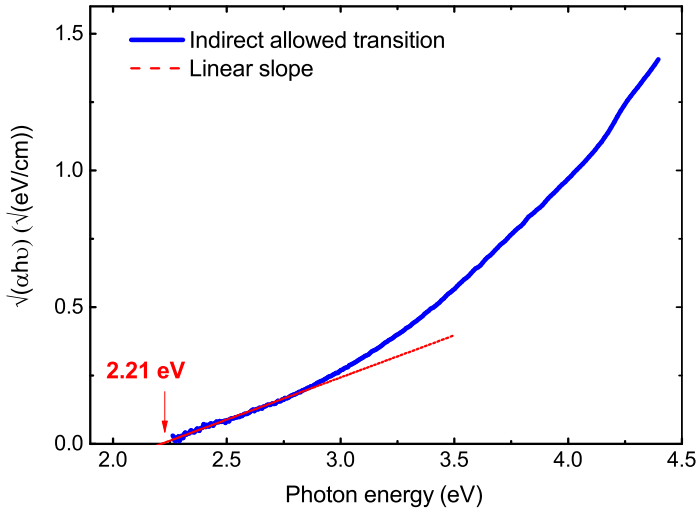

Figure S2: Tauc plot for the absorption plotted for the indirect allowed transition parameters. Linear fit of the band-edge data gives optical bandgap onset at 2.21±0.01 eV.

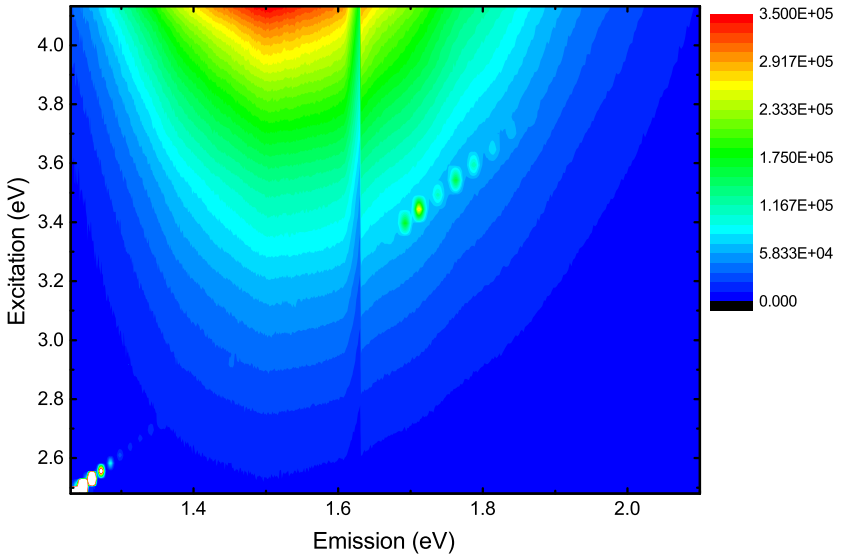

Figure S3: PLE contour map illustrates the weak dependence of the PL spectrum on the excitation wavelength. data are measured with excitation step of 5 nm between 300 nm and 500 nm.

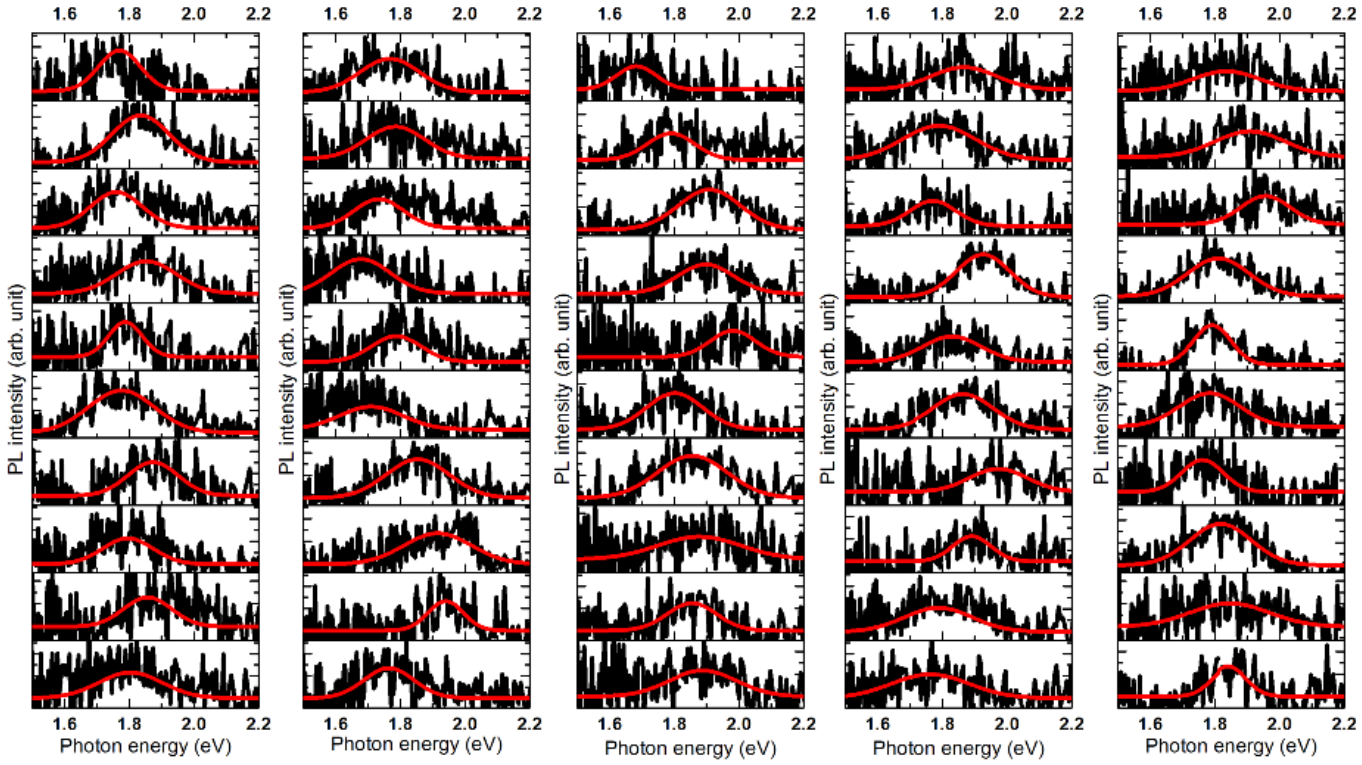

Figure S4: 50 single-NP PL spectra, fitted by a single Gaussian peak function.

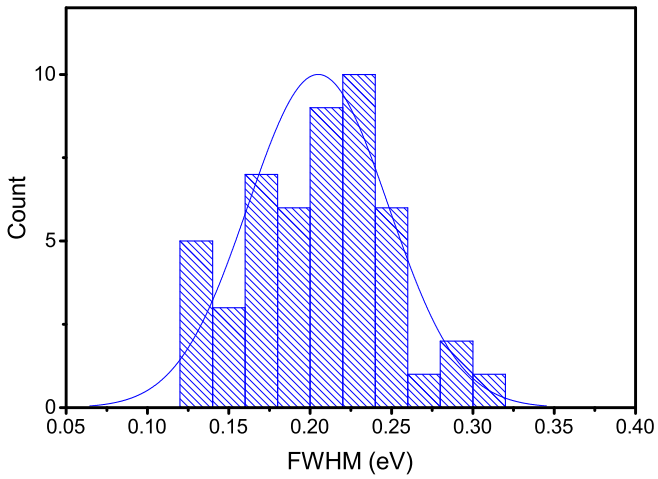

Figure S5: Histogram of the single-NP PL spectra FWHM with the mean at 205±43 meV obtained from fitting with Gaussian peak function.

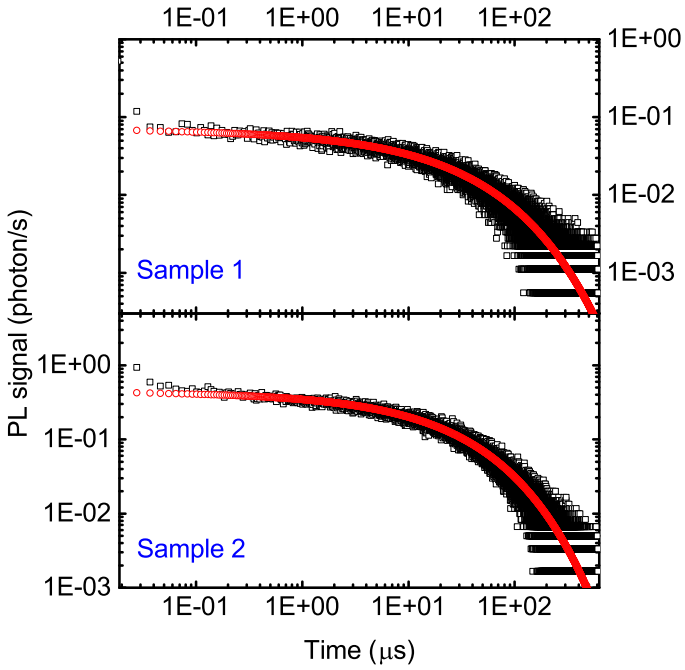

Figure S6: Time resolved PL signal of two Si-NP clusters measured without spectral resolution. Data are fitted by a stretched exponential function, giving mean lifetimes of 36.9±0.41 and 29.1±0.45 μs for the two clusters (named sample 1 and 2, respectively).

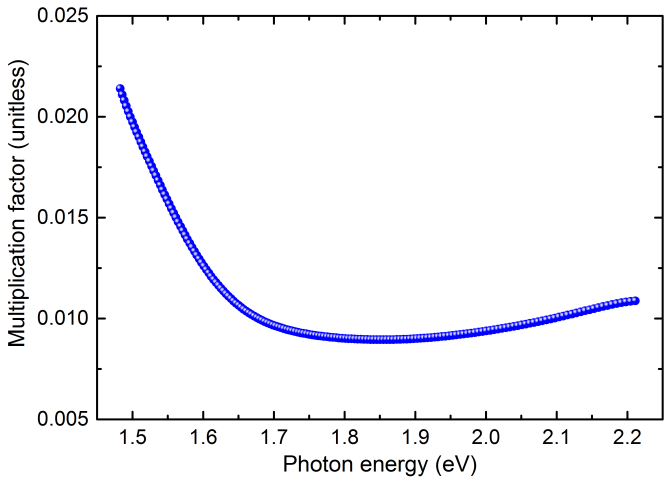

Figure S7: The single-dot spectra were implemented by the correction curve which was measured by a standard calibration tungsten lamp (Newport Corp.) with 100x oil objective, 445nm dichroic mirror, 2μm slit width, central wavelength at 750 nm, and 300g/mm grating blazed at 750 nm.

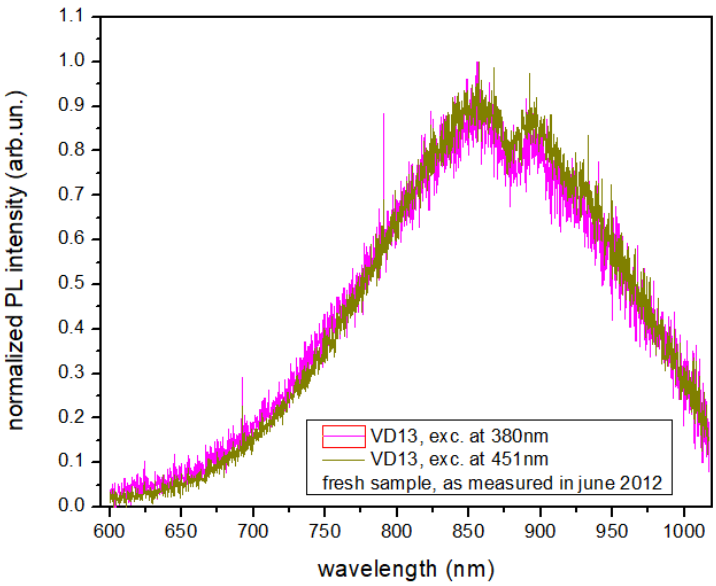

Figure S8: PL spectra of the sample measured in this work (named 'VD13' in the graph), measured in 2012 under excitation of 380 and 451 nm by a Xenon lamp in our custom built quantum yield (QY) setup. The QY was evaluated to be over 70% at the time.

Size estimation

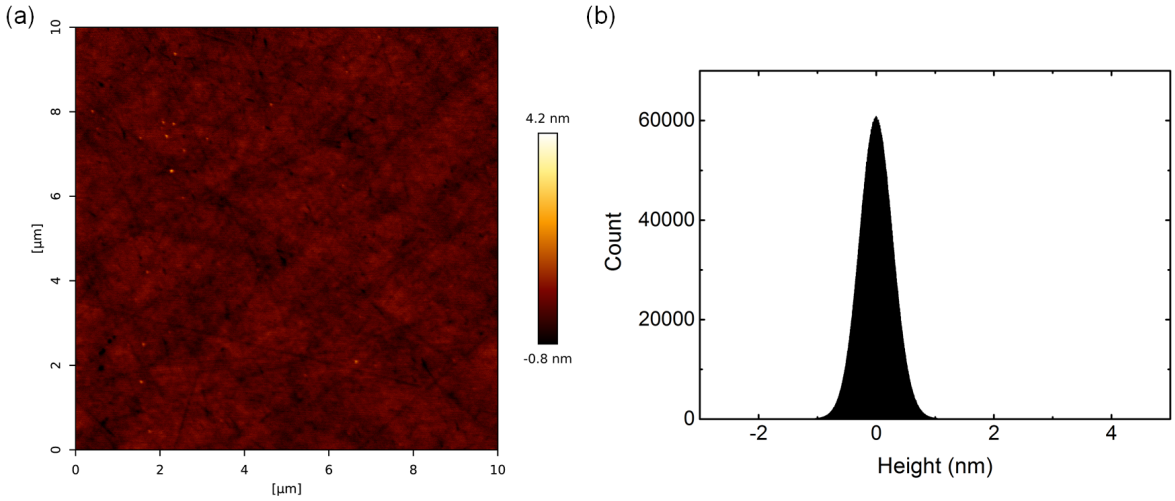

Figure S9: (a) The AFM scan of an empty quartz slide, cleaned by a water-diluted Hellmanex III solution. The scanning area is 10×10 μm^2. (b) The height histogram obtained from the AFM scan showing average height and root-mean-square (RMS) roughness of 0.0 and 0.28 nm, respectively.

Additional size evaluation could be done using XRD and Raman spectra analysis. Both methods are indirect, unlike the STEM and AFM, and do not resolve the amorphous shell thickness. Also, for small Si-NPs, more coherent synchrotron radiation XRD source should be used instead. In general, ror the XRD, various models can be used, such as Scherrer's equation[1] or Williamson-Hall equation,[2] where the latter is more precise, as it separates strain and NP size. By these methods we retrieve the mean size estimations of 17 nm and 14 nm, respectively. This is in great disagreement with the STEM, AFM and optical data we have. Interestingly, a great disagreement between the sizes estimated from TEM and XRD was observed also in study by Thiessen et al.,[3] with the greater difference for the Si-NPs with the higher amorphous content. An alternative, but also imprecise and indirect approach, is to use Raman spectra and the phenomenological model by Ritcher, Wang, and Ley (RWL model).[4] In this model, the size of the crystalline part of the NP is deduced from the bulk crystal peak shift and FWHM broadening. The estimate for the crystalline core we obtain to be 1.5-2.0 nm, which is surprisingly in line with what we expect in relation to

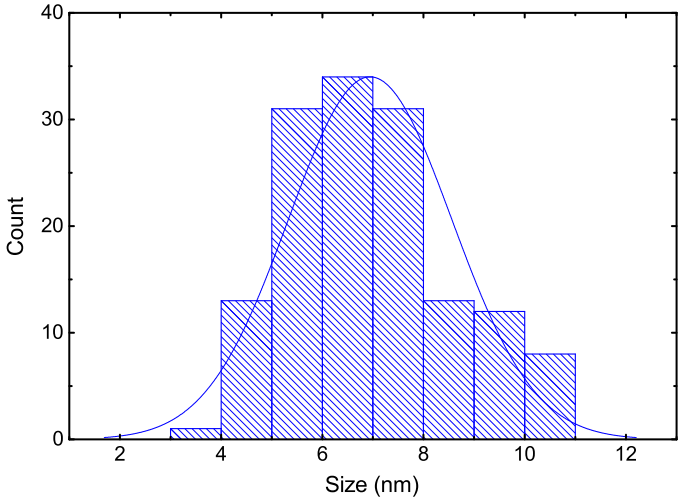

Figure S10: Histogram of Si-NPs sizes obtained from STEM measurement with the mean of 6.9±1.6 nm.

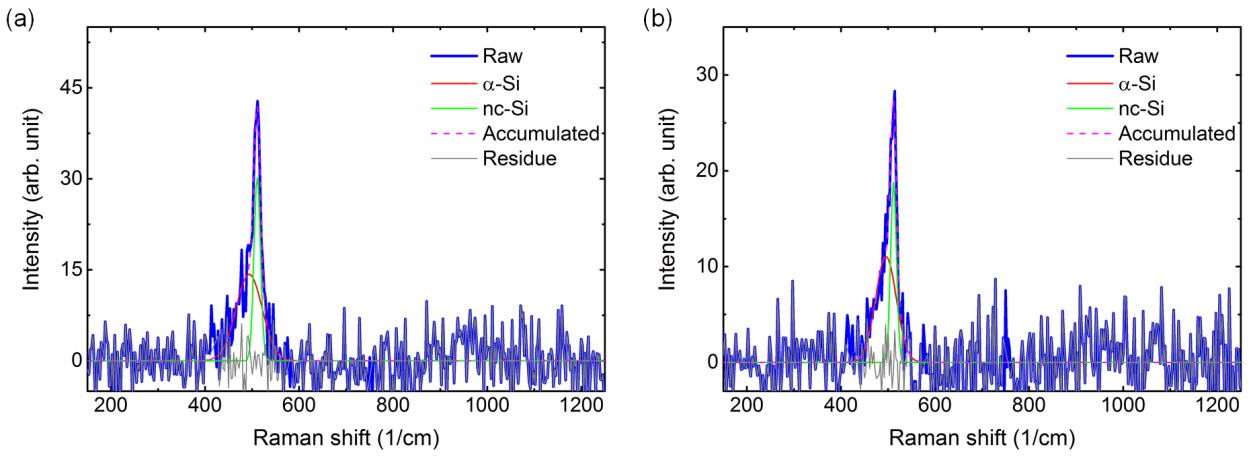

Figure S11: Raman spectra of two small Si-NP clusters depict the phonon vibration modes from crystalline Si (green line) and amorphous Si (red line) are at (a) 510.9 and 493.8, and (b) 511.8 and 495.7 cm^{-1}, respectively.

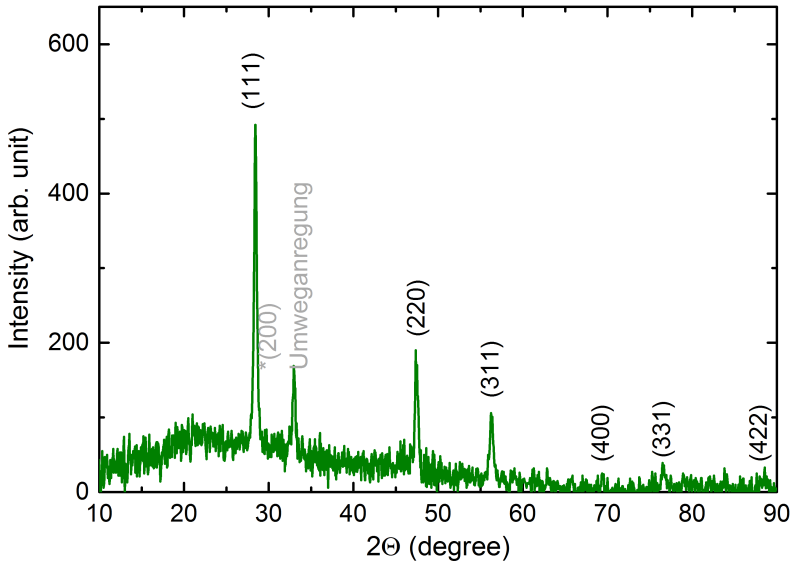

Figure S12: XRD spectrum of the ensemble of Si-NPs.

the analysis presented in[5] on a similar material. However, the RWL model was previously criticized[6] with respect to Si-NPs as well.

References

(1) Scherrer, P. Bestimmung der Größe und der inneren Struktur von Kolloidteilchen mittels Röntgenstrahlen. *Nachrichten von der Gesellschaft der Wissenschaften zu Göttingen, Mathematisch-Physikalische Klasse* **1918**, *1918*, 98–100.

(2) Williamson, G. K.; Hall, W. H. X-ray line broadening from filed aluminium and wolfram. *Acta Metallurgica* **1953**, *1*, 22–31.

(3) Thiessen, A.; Zhang, L.; Oliynyk, A.; Yu, H.; O'Connor, K.; Meldrum, A.; Veinot, J. A Tale of Seemingly "Identical" Silicon Quantum Dot Families: Structural Insight into Silicon Quantum Dot Photoluminescence. *Chem. Mater.* **2020**, *32*, 6838–6846.

(4) Richter, H.; Wang, Z.; Ley, L. The one phonon Raman spectrum in microcrystalline silicon. *Solid State Commun.* **1981**, *39*, 625 – 629.

(5) Thiessen, A. N.; Ha, M.; Hooper, R. W.; Yu, H.; Oliynyk, A. O.; Veinot, J. G. C.; Michaelis, V. K. Silicon Nanoparticles: Are They Crystalline from the Core to the Surface? *Chem. Mater.* **2019**, *31*, 678–688.

(6) Hessel, C. M.; Wei, J.; Reid, D.; Fujii, H.; Downer, M. C.; Korgel, B. A. Raman Spectroscopy of Oxide-Embedded and Ligand-Stabilized Silicon Nanocrystals. *J. Phys. Chem. Lett.* **2012**, *3*, 1089–1093.